Fatigue Crack Growth and Crack Closure Behavior of the CrNiMo Steels at Negative Stress Ratio

XIAOTIAN JING, BINGZHE LOU and FUSAN SHEN
Department of Metallic Materials Engineering, Shaanxi Institute of Mechanical Engineering, Xian, PRC

ABSTRACT

Fatigue crack growth rates and crack closure behavior of three CrNiMo high strength steels were examined at four different stress ratios ranging from R=-1.0 to R=0.5, with attention focussed on the crack closure behavior when R<0. In the latter circumstances, crack closure is lower, and a higher crack growth rate, da/dn, is observed, due to increased compressive deformation, and correspondingly less residual displacement, on crack surfaces. Fatigue crack growth rates measured at different stress ratios could be normalized in terms of the effective stress intensity range, ΔK_{eff}, in which the fracture was formed principlly by quasi-cleavage and dimpled rupture mechanisms.

KEYWORDS

Stress intensity factor, stress ratio, fatigue crack growth rate, crack closure, crack opening displacement.

INTRODUCTION

Since Elber's discovery of the fatigue crack closure phenomenon, certain important fatigue crack growth characteristics have been successfully explained on the basis of the concept of crack closure(Hollyda, 1979; Suresh et al.,1981, 1982; MaEvilly 1982). It has been demonstrated in particular that fatigue crack growth can occur only when the crack tip is fully open. The portion of the applied stress intensity range in which the crack is open has been defined as the effective stress intensity range, $\Delta K_{eff}=K_{max}-K_{op}$, where K_{max} and K_{op} are the maximun and crack opening stress intensities, respectively. When the crack closure is taken into account, ΔK_{eff} can be used instead of ΔK into Paris equation to describe the crack growth rate in the linear regime as follows:

$$da/dn = C(\Delta K_{eff})^m$$

Where C and m are material constants. This relation has been widely used to rationalize crack growth behavior in terms of the stress ratio , R(Kamai, 1984; Kobayashi, 1984). However, attention has been focussed mainly on crack growth behavior under tensile stress ratios, i.e., for R>0. There are relatively few publications discussing crack growth rate and closure bahavior at negative stress ratios(R<0). It has been reported that the crack growth rate was observed to be accelerated in aluminium alloys(Crook, 1976) and low strength steels (Okazaki, 1985) on tensile-compressive cyclic loading.

The purpose of this study is to investigate the correlation between the crack growth rate and the crack closure behavior in high strength steels when R<0.

EXPERIMENTAL

The chemical composition of the three CrNiMo steels are given in Table 1, where 40CrNiMoA is a standard commercial air-craft steel, and the other two steels, 20CrNiMoA and 80CrNiMoA, are laboratory air induction melted heats followed by consumable electrode remelting. Heat treatments and mechanical properties of the steels are listed in Table 2.

Table 1. Chemical Composition (wt.%)

Steels	C	Cr	Ni	Mo	Si	Mn	P	S
20CrNiMoA	0.17	0.54	1.76	0.23	0.24	0.80	0.02	0.005
40CrNiMoA	0.44	0.79	2.14	0.26	0.26	0.74	0.01	0.005
80CrNiMoA	0.85	0.85	1.95	0.25	0.35	0.60	0.02	0.006

Table 2. Mechanical Properties of Steels

Steels	Specimen	Heat Treatment	σ_{ys} MPa	σ_{uTs} MPa	ψ %
20CrNiMoA	A1	950/200°C	1250	2490	57.9
40CrNiMoA	B1	870/200°C	1560	2500	33.2
	B2	870/500°C	1160	2170	56.8
	B3	1200/ — °C	1310	2560	22.4
80CrNiMoA	C1	800/200°C	1850	2630	—

Fatigue crack growth tests were performed at room temperature on a servo-hydraulic fatigue test machine at room temperature, operating at the stress ratios of R=-1.0,-0.5,-0.1,0.1 and 0.5, and at a frequency of 12Hz. The shape and dimensions of the CCT specimen used in this study are shown in Fig.1. The crack length was observed by using a travelling microscope with a resolution finer than 0.01mm. The effective crack length was the mean value of four measured length examined at the two ends of the cracks on both the front and back surfaces of the specimen. The stress intensity factor, ΔK, was calculated in terms of the following

equation(Tada, 1973):

$$K = \sigma\sqrt{\pi A}\left[1-0.025(2A/w)^2+0.06(2A/w)^4\right]\sqrt{\mathrm{Sec}(\pi A/w)}$$

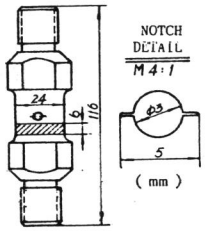

Fig.1. Test specimen

where σ is the nominal stress, A is the effective crack length and w is the width of the specimen. The measurement of th ΔK_{th} value was made by a decreasing ΔK technique until a growth rate less than 10^{-9} m/cycle was reached. The load was then raised and a ΔK-increasing test was conducted under constant load amplitude.

The crack closure behavior was examined by using an unloading elastic compliance method in which the elastic compliance was electronically subtracted from the total crack opening displacment signal (Kikukawa, 1977). The displacement transducer mounted on the central hole was a specially made crack mouth clip gauge used for the central crack measurement.The load-displacement signal was recorded at a low test frequency f=0.1Hz. The value of the cyclic crack opening load, P_{op},was determined at the deflection point on the curve obtained, and thereby the effective stress intesity factor, ΔK_{eff}, and the crack opening coefficient, U, were computed as follows:

$$\Delta K_{eff} = \begin{cases} K_{max} - K_{min} & (K_{op} \leqslant K_{min}) \\ K_{max} - K_{op} & (K_{op} > K_{min}) \end{cases}$$

$$U = \begin{cases} \Delta K_{eff}/\Delta K & (R > 0) \\ \Delta K_{eff}/K_{max} & (R \leqslant 0) \end{cases}$$

After the fatigue test was finished, specimens were pulled apart, and one half of the fractured specimens were examined under the SEM. The other halves were nickel plated and the fracture profiles and microstructures were observed under the optical microscope.

RESULTS AND DISCUSSION

Crack Closure Behavior At Different Stress Ratios

The relation between the crack growth rate, da/dn, and the stress intensity range,ΔK, for four stress ratios examined in the 40CrNiMoA steel(B1) is illustrated in Fig.2. It shows that da/dn is accelerated by increasing the stress ratio, R, either in positive(R>0) or negative(R<0) stress ratios. The value of ΔK_{th} decreases as R increases. The da/dn-ΔK curves in the linear regime for different stress ratios demonstrate almost the same slope with the value of constant m at 2.02. The value of ΔK_{th} which is around 6.8-7.2 MPa$\sqrt{m}$ at the negative stress ratios used in this investigation goes down to 5.0 MPa$\sqrt{m}$ at a stress ratio of R=0.1.

In Figure 3, experimental results are er-plotted and the variation of the fatigue crack growth rate, da/dn, is shown as a function of maximum stress intensity, K_{max}. The tested values of da/dn in the linear regime obtained at various stress ratios fall eventually in a narrow zone where the value of da/dn for negative cyclic loadingis about 1.45 times as high as that for tensile cyclic loading. The fatigue crack growth rate in near-threshold region decerases as R increases and values of $(K_{max})_{th}$, however, are increased with the stress ratio from 3.5 MPa$\sqrt{m}$ for R=-1.0 and 4.7 MPa$\sqrt{m}$ for R=-0.5 to 5.6 MPa$\sqrt{m}$ for R=0.1.

The result shown in Fig.3 indicates that the K_{max} is one of the dominating factors for the fatigue crack growth in the linear regime. It can also be seen that the acceleration in the fatigue crack growth rate and the depression in the ΔK_{th} in this tested high strength steel are not as evident as those demonstrated in the low strength steel(Okazaki, 1985). The difference in the behaviors may be arised from the great difference in the yield strengths of tested materials. It is reasonable to expect that a higher strength of the material leads to a smaller compression on crack surfaces, and therefore only a slight variation in crack growth rate could be detected in high strength materials subjected to different negative stress ratios.

The crack closure response of 40CrNiMoA steel at various stress ratios is given in Fig.4. The crack opening coefficient, U, is found to be independent of the K_{max} in the linear regime while it decreases rapidly as the K_{max} decreases down to the near-threshold region which is associated with a higher crack closure (MaEvily, 1982; Bingnonoennt, 1985). It is interesing to note that the value of U varies non-monotonically with the stress ratio. This implies that the positive stress ratios cause a higher closure on crack surfaces than the negative stress ratios and thus cause a smaller residual displacement. The higher crack closure is probably associated with a greater compression on the crack surfaces due to the coersive crack closure made by the applied compressive stress and a smaller residual displacement. The SEM examination has proved that greater pressed marks were observed on crack surfaces of the specimen subjected to a negative stress ratio, as shown in Fig.5a, in comparison with the features shown in Fig.5b, which were formed under a positive stress ratio. The compressive deformation produced by the coercive closure on crack surfaces at negative stress ratio reduces obviously the residual displacement and hence the plasticity induced crack closure.

In order to evaluate the effect of crack closure on da/dn, the crack growth data can be re-arranged on the basis of the effective stress intensity range, ΔK_{eff}. The experimental data are found to fall in a narrow strip as the hatched zone in Fig.3, and the influence of the stress ratio on da/dn and ΔK_{th} is then eliminated. It is evident that all the crack growth data can be normalized according to ΔK_{eff} when the crack closure phenomenon is considered. The variation of the da/dn as a function of ΔK_{eff} can be expressed by a formula as follows:

$$da/dn = 2.21X10^{-10}X(\Delta K_{eff})^{2.02} \qquad [m/cycle]$$

The correlation coefficient of this expression is greater than 0.997.

The Effect Of Strength On Crack Growth And Crack Closure

Figure 6 shows the relation between the crack growth rate, da/dn, and the stress intensity range, ΔK, for 40CrNiMoA steel treated at different conditions. Crack growth rates for three conditions are very close to one another the m value being at 2.24. The ΔK_{th} values for condition B2 and B3, however, are seen to be lower. It can be seen from Fig.6 that condition B1 with the highest strength is observed to have the lowest da/dn value in the linear regime at R=-1.0. The acceleration of da/dn in linear regime is more obvious for condition B2 with lower strength as compared with B1. The B3 with intermediate strength, however, shows the highest da/dn in spite of the fact that its coarse grain size be benificial to the roughness induced crack closure (Suresh, 1981). The anomalous acceleration of da/dn for B3 can be attributed to the intergranular fracture mechanism, as shown in Fig.7 and Fig.8, which balances the potentially benificial effect caused by roughness induced crack closure. This is proved by the fact that the slope of the da/dn-ΔK curve goes up when ΔK>40 MPa$\sqrt{m}$ because of much larger percentage of intergranular fracture appearing on the fracture surface.It should be pointed out that the crack growth rate for all the three condition can be completely normalized into a single line as shown in Fig.6.

The data of the fatigue crack growth rate for the three CrNiMo steel operated at a stress ratio of R=-1.0 is shown in Fig.9. Crack growth rates in the linear regime for 20CrNiMoA and 40CrNiMoA are almost the same. The teated high carbon steel, 80CrNiMoA, exhibits a much higher crack growth rate and a lower threshold stress intensity, ΔK_{th}, due to the higher strength. The crack closure response at R=-1.0 for the three tested steels is shown in Fig.10 where the crack opening stress, S_{op}, and the ratio of K_{op}/K_{max} are plotted versus the maximum stress intensity, K_{max}, respectivelly. The S_{op} is found to increase with the strength or/and the carbon content of the steel and all data obtained here are much higher than S_{op}=0 MPa for HT-55 steel reported by Okazaki(1985). It illustrates that a higher carbon content or a higher strength gives rise to a stronger resistance to the compressive deformation on crack surfaces and makes for an early closure on unloading. It can also be seen from Fig.10b that K_{op}/K_{max} increases rapidly with the decrease in K_{max}.

Experimental results for three tested steels at R=-1.0 can be also well normalized into a straight line in the da/dn-ΔK_{eff} diagram as shown in Fig.9, while the 80CrNiMo steel is a exception which exhibits a different fracture mechanism. This means that the difference in da/dn due to the variation of the strength or/and the carbon content of the steel can be explained by using the concept of the crack closure so long as the fracture is mainly composed of quasi-cleavage and dimpled rupture mechanisms. Therefore, the ΔK_{eff} is believed to be the dominating factor for the crack growth.

The fracture mechanism is still considered to be an important

factor that should not be ignored owing to the fact that it affects the micro-ductility of materials and the residual displacement on crack surfaces(Kikukawa, 1979), and that it affects the crack growth resistance. The crack closure approach is successful in the explanation of the variation in da/dn only when the first effect dominates, such as in the case where the quasi-cleavage and the dimpled rupture fracture prevails as shown in this study as well as where the striation mechanism dominates(Fleck, 1984). However, the crack closure approach would be invalid if the second effect is a more important factor, such as the behaviors shown by 80CrNiMoA and 40CrNiMoA(B3) steels.

CONCLUSIONS

With the increase in the stress ratio, R, the fatigue crack growth rate, da/dn, increases and the threshild stress intensity ΔK_{th}, decreases, while the effective stress intensity range, ΔK_{eff}, changes non-monotonically.

An acceleration of da/dn at negative stress ratios was exhibited in high sterngth CrNiMo steels due to the decrease in the plasticity induced crack closure resulted from the compressive deformation on the crack surfaces, although it is not as evident as that shown in low strength steels.

The crack growth rates at positive and negative stress ratios can all be well normalized as:

$$da/dn = 2.21X10^{-10} X (\Delta K_{eff})^{2.02} \qquad [\,m/cycle\,]$$

when the fracture is mainly composed of the quasi-cleavage and dimpled rupture mechanism. The ΔK_{eff} is believed to be the most important factor affecting the crack growth rate.

REFERENCES

Bingnonnet, B., Dias, A. and H.P. Lieurade(1984). Advances in Fracture Research, Pergamon Press, p.1861.
Crook, T.W. (1976). Trans. ASME ser. B, 28, 893.
Elber, W. (1971). ASTM STP 486, 230.
Fleck, N.A. (1984). CUED/C-MATS/TR, 104.
Holliday, M.D and C.J. Beevers (1979). Int. J. Fracture, 15, R27.
Kikukawa, M., M. Juno and K. Tanaka (1976). Proc. ICM2, Boston, 254.
Kobayashi, H., T. Ogawa, H. Nakamura and H. Nakazawa (1984). Advances in Fracture Research, Pergamon Press, p. 2481.
Komai, K., S. Murayama and H. Kanasaki (1984). Advances in Fracture Research, Pergamon Press, p. 2489.
McEvily, A.J. and K. Minakawa (1982). Strength of Metals and Alloys, edited by R.C. Gifking, Pergamon Press, Oxford and New York.
Okazaki, Y. (1985). Journal of Materials (in Japanese), 34, 1167.
Tada, H., P.c. Paris and G.R. Irwin (1973). The Stress Analusis of Crack Handbook, Del Research Corp, Heller town, Pa.
Suresh, S. and R.O. Ritchie (1981). Metall. Trans., 12A, 1435.
Surech, S. and R.O. Ritchie (1982). Metall. Trans., 13A, 1627.

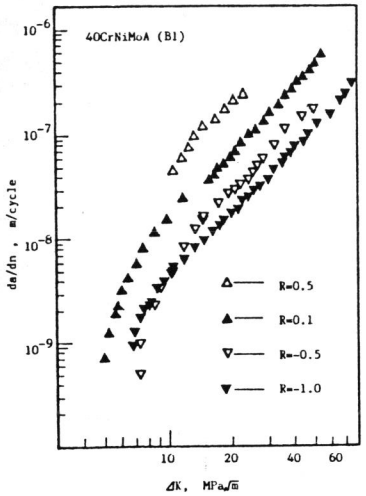

Fig.2. da/dn-ΔK curve for 40CrNiMoA steel(B1)

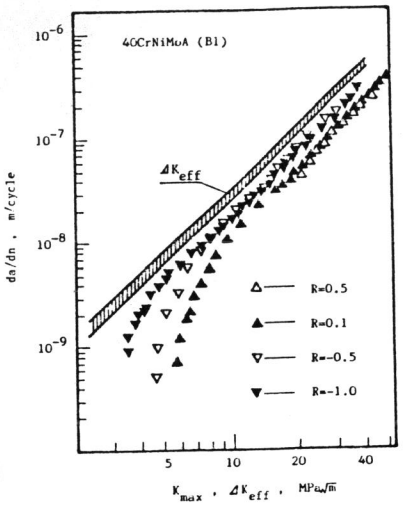

Fig.3. da/dn-K_{max}, ΔK_{eff} for 40CrNiMoA steel(B1)

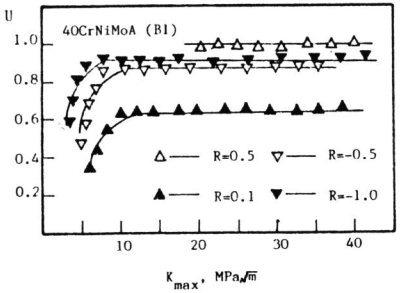

Fig.4. U-K_{max} curve for 40CrNiMoA steel(B1)

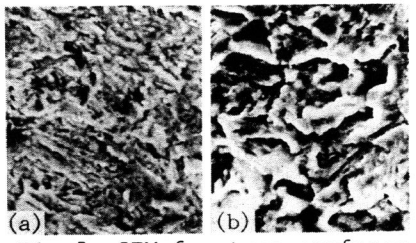

Fig.5. SEM fracture surfaces of 40CrNiMoA steel(B1) (a) R=-1.0; (b) R=0.1.

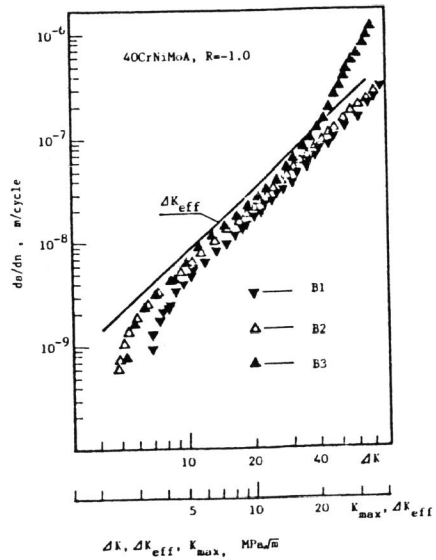

Fig.6. da/dn-ΔK, K_{max}, ΔK_{eff} for 40CrNiMoA steel

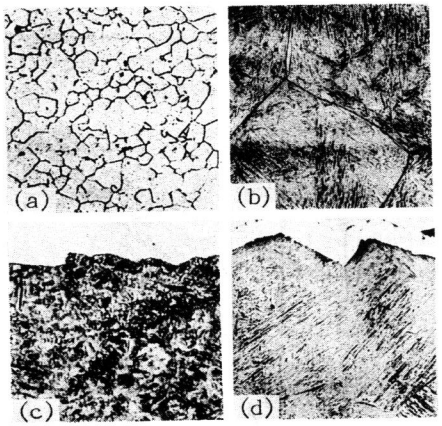

Fig.7. Metallographic photos showing grain sizes & fracture profiles:
(a) grain size for (B1), X200;
(b) grain size for (B3), X200;
(c) fracture profile (B1), X600;
(d) fracture profile (B3), X170.

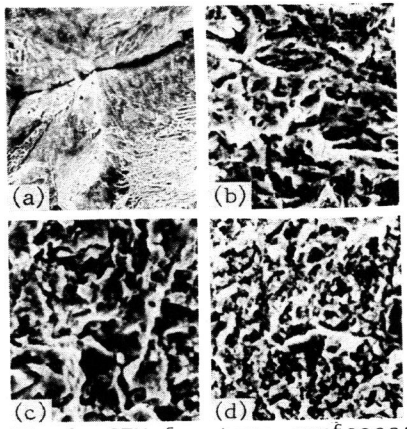

Fig.8. SEM fracture surfaces:
(a) 40CrNiMoA (B3), X260;
(b) 20CrNiMoA (A1), X1500;
(c) 40CrNiMoA (B1), X1500;
(d) 80CrNiMoA (C1), X1500.

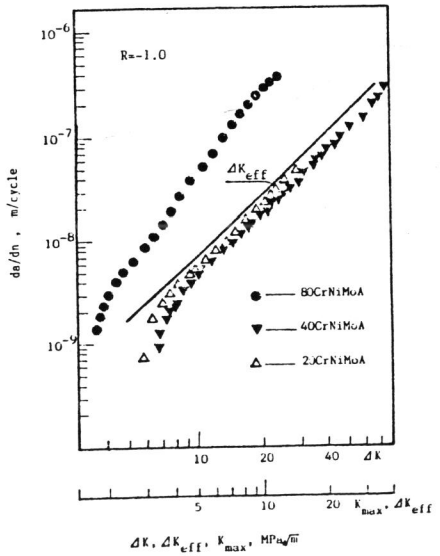

Fig.9. da/dn-ΔK, K_{max}, ΔK_{eff} for three tested steels

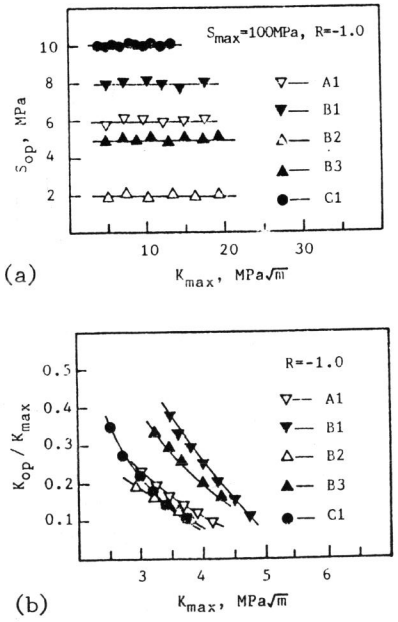

Fig.10. Crack closure responses for tested steels: (a) S_{op}-K_{max}; (b) K_{op}/K_{max}- K_{max}